Urania
Jurnal Ilmiah Daur Bahan Bakar Nuklir

Beranda jurnal: https://ejournal.brin.go.id/urania/

COMPARATIVE STUDY OF RADIATION HARDNESS IN SEMICONDUCTOR MATERIALS (Si, SiC, GaN, DIAMOND) FOR AMERICIUM-241 WASTE-BASED NUCLEAR BATTERIES

Pribadi Mumpuni Adhi[1*], Millaty Mustaqima[2]
[1]Magister Terapan Rekayasa Teknologi Manufaktur, Politeknik Negeri Jakarta,
Jl. Prof. G. A. Siwabessy, Kampus UI, Depok, Jawa Barat 16425
[2]Physics Study Program, Faculty of Military Mathematics and Natural Sciences,
Indonesian Defence University, Kawasan IPSC, Sentul Bogor, Jawa Barat 16810
*e-mail: pribadi.adhi@mesin.pnj.ac.id

(Submitted: 07–02–2026, Revised: 02–04–2026, Accepted: 06–04–2026)

ABSTRACT

COMPARATIVE STUDY OF RADIATION HARDNESS IN SEMICONDUCTOR MATERIALS (Si, SiC, GaN, DIAMOND) FOR AMERICIUM-241 WASTE-BASED NUCLEAR BATTERIES. Using Americium-241 (Am-241) radioactive waste from spent smoke detectors as an alpha-voltaic energy source provides a long-term power solution for sensors in extreme environments. However, high-energy alpha particles (5.48 MeV) are inherently destructive to semiconductor crystal structures. This study aims to identify the optimal Wide Bandgap (WBG) material by analyzing energy-loss mechanisms (stopping power), lattice damage, and device geometry design parameters. SRIM 2013 simulations were performed on Si, SiC, GaN, and diamond targets. The analysis includes ion distribution range, electronic and nuclear stopping profiles, the calculation of a Radiation Tolerance Index, and the determination of minimum active thickness (T_{min}) based on projected-range statistics. The results show that diamond exhibits the highest tolerance index of 670, enabling the thinnest device design (~15 µm). In contrast, silicon requires nearly twice the active thickness (~28 µm) and suffers the most severe structural damage. Silicon carbide (SiC) is recommended as a cost-effective alternative with a Radiation Tolerance Index of 593. While diamond is the superior material for space-constrained applications, SiC offers the best balance between radiation resistance and cost for terrestrial applications.

Keywords: Alpha-voltaic, Americium-241, nuclear battery, SRIM

INTRODUCTION

Management of spent nuclear fuel waste is a significant challenge in the nuclear fuel cycle, particularly in ensuring long-term safety and minimizing radiological impacts on the environment. Dry cask storage systems are studied as solutions for this [1]. In the Indonesian context, specific designs of dry casks with air gaps have been analyzed to ensure criticality safety for the storage of spent fuel from the proposed Non-Commercial Power Reactor (RDNK) [2]. Concurrently, the management of Disused Sealed Radioactive Sources (DSRS) is a critical priority. Global empirical assessments highlight the Borehole Disposal (BHD) system as a robust safety solution for such waste [3]. This concept is actively being evaluated for implementation in the Serpong Nuclear Area, where site characterization and safety assessments have demonstrated its suitability for the secure isolation of DSRS [4].

Americium-241 (Am-241) is a byproduct of the nuclear fuel cycle, originating from the radioactive decay of Plutonium-241. While often viewed as a byproduct, its potential value is significant; for instance, previous research has demonstrated its capability to enhance the performance of mixed-oxide nuclear fuels [5]. Beyond this application, Am-241 is widely utilized commercially in ionization-type smoke detectors. However, disposing of these devices creates a significant inventory of radioactive waste, with high handling costs. Instead of mere disposal, this study proposes valorizing Am-241 waste into long-life micropower sources—a promising approach that nonetheless presents significant material challenges [6], [7].

These micropower sources, essentially functioning as nuclear batteries, utilize alpha particles with high kinetic energy (~5 MeV) and significant mass, making them highly destructive to converter materials [8]. If conventional semiconductor materials such as silicon, commonly used in computer chips, are used as a medium for energy conversion, their crystal structure will be damaged by displacement damage before the alpha energy potential can be utilized optimally [7], [9]. Therefore, the development of alpha-particle-based nuclear batteries requires materials with high radiation hardness that maintain structural stability and electronic properties under intense radiation exposure, as reported in recent studies [10], [11].

In response to the need for high-radiation-hardness materials, wide-band-gap (WBG) semiconductors are a promising candidate for alpha-particle-based nuclear batteries. Among various WBG materials, silicon carbide (SiC) and gallium nitride (GaN) are chosen [12], [13] because their technologies are cost-effective and widely used for fast charging of cell phones and electric cars [14]. SiC not only excels commercially but also offers greater radiation hardness than conventional silicon, especially in maintaining structural stability under heavy particle irradiation [15]. On the other hand, diamond is also an ideal comparison since it excels in mechanical and electrical properties, including its high atomic binding energy [16] and its extraordinary radiation hardness, as reported in [17].

The main challenge in utilizing alpha particles lies in their large mass, which causes their energy to be lost through two competing stopping mechanisms: electronic stopping (S_e) and nuclear stopping (S_n). Electronic stopping involves interactions with the electron cloud that produce ionization without damaging the crystal lattice, while nuclear stopping involves direct collision with atomic nuclei that cause displacement damage in the form of vacancies and other defects that permanently damage the crystal structure [18]. In the specific case of nuclear batteries, these structural defects lead to a permanent degradation of the device's conversion efficiency and electrical output [19], [20].

The competition between these two mechanisms depends on the particle's kinetic energy and the properties of the target medium. For example, simulation studies for Am-241 alpha particles with energies of approximately 5.48 MeV in GaN show that most of the energy is deposited through electronic stopping, while the direct contribution to the lattice through nuclear collisions is much smaller, although defects remain if the atomic recoil energy exceeds the material's displacement energy [21]. However, literature quantitatively describing the contribution ratio between these two stopping mechanisms (S_e/S_n) specifically at an alpha energy of 5.48 MeV in WBG materials remains relatively scarce, which is the focus and novelty of this study.

In this study, a computational evaluation of alpha-particle interactions with Si, SiC, GaN, and Diamond was conducted

using energy-loss analysis and particle-penetration profiles. The evaluation results were used to determine the optimal device thickness, enabling the device design to minimize material usage without sacrificing radiation shielding capabilities or performance stability under alpha particle exposure.

METHODOLOGY

a. Simulation Configuration

The ion simulation transport was performed by using the SRIM 2013 code [22]. In this simulation, we used the ion distribution and the calculation damage method. This method utilizes the Modified Kinchin-Pease formalism model to estimate lattice vacancies and displacement [23]. This approach was chosen to optimize computational efficiency while maintaining statistical accuracy for crystalline materials, compared to the Cascade mode.

High-energy ions, 5.48 MeV, were chosen as the radiation source from Helium-4 (an alpha emitter). This energy was selected due to the characteristics of the primary alpha decay peak of the isotope Am-241, which has a high probability of transition of 85.2% [24]. The incident angle was to be 0° toward the target surface. For each material, the simulation was conducted using 5,000 incident ions.

Four target materials were selected: Si, SiC, GaN, and diamond. Table 1 presents the density of each material. The thickness of the target material layer was set to 30 μm to capture the entire ion track.

Table 1. Density of target material

Name	Density (g/cm^3)
Si	2.32
SiC	3.21
GaN	6.15
Diamond (C)	3.52

b. Data Analysis Method

Four output files were extracted from the SRIM 2013 simulation results: RANGE.txt, IONIZ.txt, PHONON.txt, and VACCANCY.txt. For the comparison of ion distribution data, we plotted the penetration range and the ion distribution from the file RANGE.txt.

To quantify the inherent resistance of each material to alpha-particle-induced damage, we introduced a Radiation Tolerance Index (R), defined as the ratio of the total electronic energy loss S_e to the total nuclear energy loss S_n over the entire ion trajectory. We extracted the electronic stopping power S_e from the IONIZ.txt output file and the nuclear stopping power S_n from the PHONON.txt file. Then, the radiation tolerance index (R) was calculated by using equation (1). To evaluate structural damage, we calculated the total vacancies/ion for each material using data from VACCANY.txt. Finally, to design the geometry with the safety margin, the minimum thickness T_{min} can be determined by using equation (2). Where R_p is the projected range extracted from the Ion Average Range in the RANGE.txt file, this data refers to the penetration distance (depth) and determines how thick the battery must be designed to be. In a normal distribution, 3σ encompasses 99.7% of the population. This means that, with this thickness, we ensure that 99.7% of alpha particles are completely stopped within the material.

$$R = \frac{\int S_e \, dx}{\int S_n \, dx} \quad (1)$$

$$T_{min} = R_p + 3\sigma \quad (2)$$

RESULTS AND DISCUSSION

a. Comparison of Projected Range

Figure 1 shows the comparison of the ion distribution range (Bragg Peak) between Si, SiC, GaN, and Diamond. From the graph, we can see that Diamond and GaN have a shorter penetration depth than the other two materials. The shorter penetration depth means better stopping power. Diamond and GaN have a range for stopping alpha radiation around 14-15 μm, whereas Si has a more extended range around 28 μm.

This penetration depth represents the projected range R_p. High-density materials generally have higher stopping power; therefore, an ion can stop over a shorter range. Si has a lower density compared to diamond. Since diamond is denser than Si, diamond can stop ions faster than Si. However, an inverse relationship is observed between penetration depth and peak height. Diamond has the highest peak, more than 25,000 ions/cm3, while Si has the lowest peak, around 13,000 ions/cm^3. This phenomenon arises because the stopping volume is narrower in denser materials. Consequently, when ions are confined to a very short stopping range (as in diamond), the ion concentration per unit volume becomes

 DOI: https://doi.org/10.55981/urania.2026.14937

significantly higher. Conversely, in silicon, ions are distributed over a larger depth, leading to a reduced peak concentration.

The silicon curve (blue line) exhibits the widest distribution, while the diamond curve (red line) is sharp and narrow, a phenomenon referred to as straggling. As ions propagate farther within a material (e.g., silicon), they experience more random collisions, leading to greater statistical variation in their stopping positions and a broader distribution. In contrast, the shorter penetration distance in diamond results in reduced variation and a correspondingly sharper peak.

This Figure 1 graph highlights the contrast between conventional silicon and WBG materials, including SiC, GaN, and diamond. Diamond and GaN provide more effective radiation shielding per unit thickness than silicon due to their shorter ion stopping ranges. These results have important implications for engineering design. The use of diamond or GaN enables a thinner, more compact battery design compared with silicon.

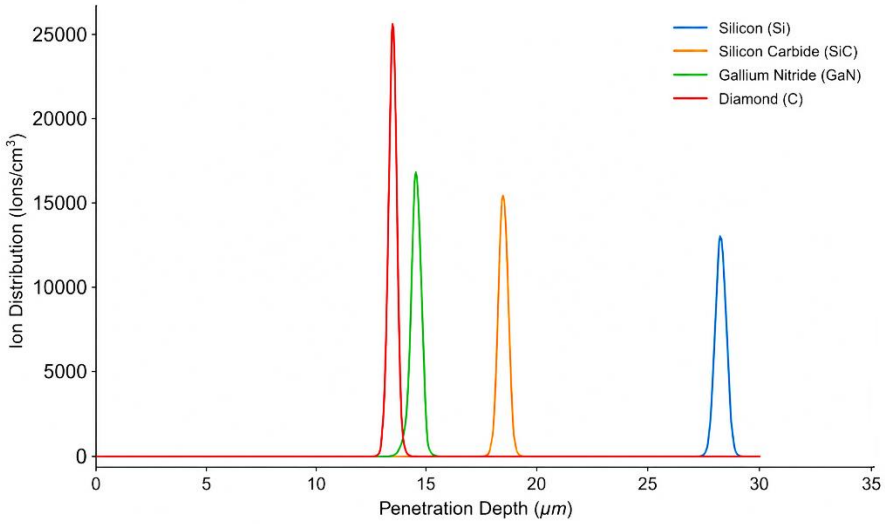

Figure 1. Comparison of the ion distribution range

b. Energy Loss Mechanism

Figure 2 illustrates the ion energy loss rate (dE/dx) during ion penetration through the four materials. Across all four graphs, the solid-line curve (S_e) clearly dominates the dashed-line curve (S_n). The S_e value increases with penetration depth, reaching a maximum at the Bragg peak, before sharply decreasing to zero. This occurs because, at high energies, ion energy loss is dominated by inelastic interactions with the target electron cloud (excitation and ionization), rather than by nuclear collisions.

Diamond has the highest stopping power, with a peak energy loss of around 68 eV/Å. Materials with higher electron density (such as diamond) provide greater resistance or braking force to ions as they traverse. Because diamond dissipates ion energy much more rapidly, the ions come to rest over a shorter distance (~13 µm) than in silicon, which dissipates only 34 eV/Å and stops the ions at approximately 28 µm.

The dashed-line curve S_n in Figure 2 remains close to zero throughout most of the ion trajectory and exhibits only a minor rise near the end of the track, at the maximum penetration depth. This occurs because nuclear stopping, elastic collisions with target atomic nuclei, becomes dominant only when the ion velocity is very low. As a result, crystal structural damage caused by nuclear collisions is concentrated near the end of the ion trajectory. Along the initial path, the damage is predominantly electronic in nature (ionization and heating), whereas physical crystal damage accumulates in the Bragg peak region.

The solid-line curve S_e in Figure 2 exhibits a non-linear curve, increasing gradually and peaking near the end of the ion path. This behaviour represents a classic Bragg curve characteristic. As ions decelerate, their interaction cross-section with electrons increases, resulting in a higher energy transfer rate (dE/dx) near the end of the path.

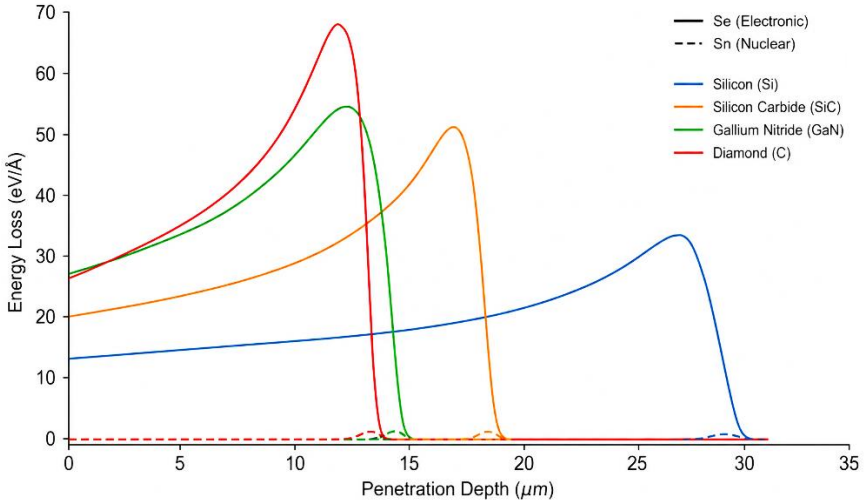

Figure 2. Comparison of the ion distribution range

c. Radiation hardness

This bar chart in Figure 3 presents the Radiation Tolerance Index. A higher ratio (taller bars) indicates that electronic interactions dominate ion energy loss, minimizing energy transfer to lattice damage. As a result, diamond (value of 670) theoretically exhibits the lowest structural damage per unit of deposited energy among the materials studied. Based on the graph, diamond exhibits the highest index value (670), significantly exceeding silicon (546) and GaN (430). This confirms the diamond's status as a radiation-hard material. Because the constituent carbon atoms in diamond are very light ($Z = 6$). The probability of nuclear scattering, S_n, is relatively small compared with its powerful electronic interaction, S_e, as shown in Figure 2. This makes diamond highly suitable for radiation detectors operating in extreme environments, as the sensor is less prone to rapid degradation

However, GaN shows the lowest ratio (430), even lower than silicon (546), which presents an interesting discussion point. Despite being known as a radiation-hard material due to its strong bonding, the low S_e/S_n ratio arises from the presence of heavy gallium atoms (Z=31), which have a larger nuclear collision cross-section and thus increase S_n. While GaN absorbs more atomic energy, its practical radiation resistance is often mitigated by a high displacement threshold energy. However, this analysis shows that GaN statistically receives the most significant proportion of damaging nuclear energy.

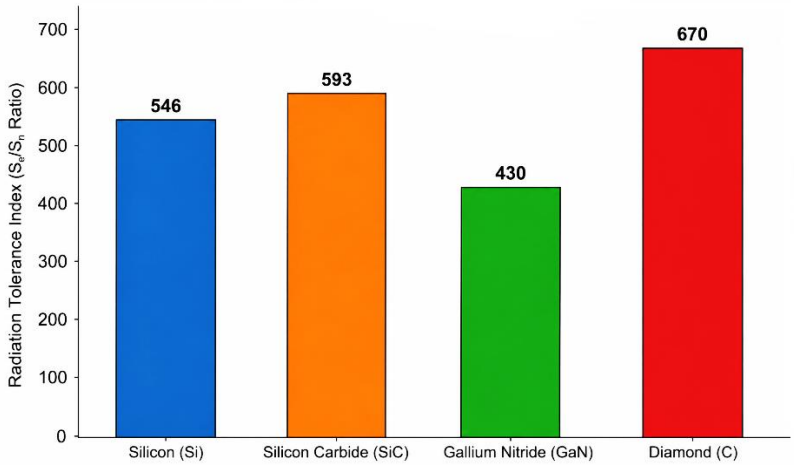

Figure 3. Radiation Tolerance Index between Si, SiC, GaN, and Diamond

 DOI: https://doi.org/10.55981/urania.2026.14937

Meanwhile, SiC shows a well-balanced performance. it exhibits better radiation resistance than conventional silicon (higher ratio), supporting the use of SiC in power electronics for satellites or nuclear reactors, where component lifetime is strongly dependent on the accumulation of atomic damage.

d. Total Vacancies

The bar chart in Figure 4 shows the total vacancies per ion, defined as the average number of vacancy defects produced by a single ion as it traverses the material. This parameter serves as a direct indicator of radiation damage.

Si exhibits the most severe damage, generating approximately 241 vacancies per ion, which confirms its relatively low resistance to high-energy alpha-particle bombardment. In contrast, diamond shows the lowest level of structural degradation, producing only 87 vacancies per ion. This represents nearly a threefold reduction in defect formation compared with silicon. The significantly lower vacancy production in diamond is consistent with its high Radiation Tolerance Index, in which ion energy loss is predominantly governed by electronic interactions rather than by damaging nuclear collisions. These results clearly demonstrate that the crystal structure of silicon is substantially more susceptible to permanent displacement damage. In contrast, diamond offers superior intrinsic radiation hardness, making it a highly promising material for long-lived nuclear battery and radiation-tolerant device applications.

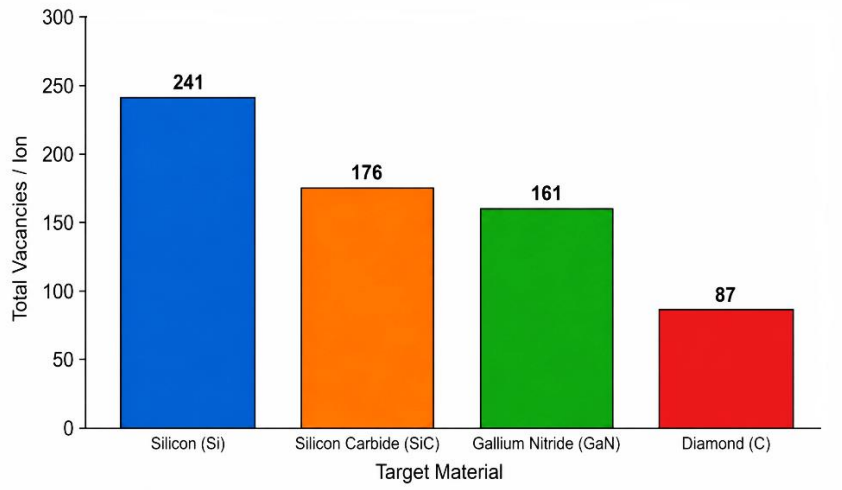

Figure 4. Total Vacancies/ion between Si, SiC, GaN, and Diamond.

To create a single vacancy, the energy transferred from the incident ion to a target atom must exceed the Displacement Threshold Energy (E_d). Diamond possesses powerful and short sp^3 covalent bonds, resulting in a very high displacement threshold energy, typically in the range of 40–50 eV [25], [26], [27]. This indicates that carbon atoms are highly resistant to being displaced from their lattice sites. In contrast, silicon has weaker atomic bonding with a much lower E_d value, approximately 15–20 eV [28]. Consequently, ion collisions with the same energy are more likely to displace silicon atoms, leading to a significantly higher number of vacancy defects.

SiC (176) and GaN (161) occupy an intermediate position. They generate significantly fewer vacancies than silicon, yet still produce approximately twice as many vacancies as diamond. This indicates that although WBG materials such as SiC and GaN offer superior radiation resistance compared with conventional silicon technology, diamond remains the best material for extreme applications where crystal integrity is the primary priority.

e. Design Geometry

Figure 5 presents the recommended minimum substrate thickness required to ensure that the entire ion energy is fully absorbed within the active material. This thickness is calculated from the mean projected range (R_p) combined with a safety margin of 3σ.

Si requires the thickest substrate, approximately 29.8 µm. This is attributed to its lower stopping density and broader straggling effect, which necessitate a thicker safety margin to prevent ion escape. In contrast, materials such as diamond and GaN exhibit superior stopping capability. Diamond requires a total thickness of only 14.1 µm, while GaN requires 15.6 µm. From a practical perspective, this indicates that using WBG materials such as diamond or GaN results in approximately 45–50% reduction in material volume for the same energy absorption function. This volumetric efficiency is particularly critical given the high fabrication cost of high-quality single-crystal materials.

Compared with Si, the use of diamond enables a reduction in device thickness of more than 50%, from approximately 30 µm to around 14 µm. The thinner device geometries achievable with diamond and GaN enable more efficient implementation of multi-layer or stacked architectures. Within the same physical space occupied by a single silicon cell (~30 µm thick), engineers can stack two diamond cells (2 × 14 µm). By stacking two cells in series within the same volume, the output voltage (open-circuit voltage) can be effectively doubled without increasing the overall packaging dimensions. Therefore, Figure 5 recommends transitioning to WBG materials not only for enhanced radiation tolerance but also to maximize energy density per unit volume.

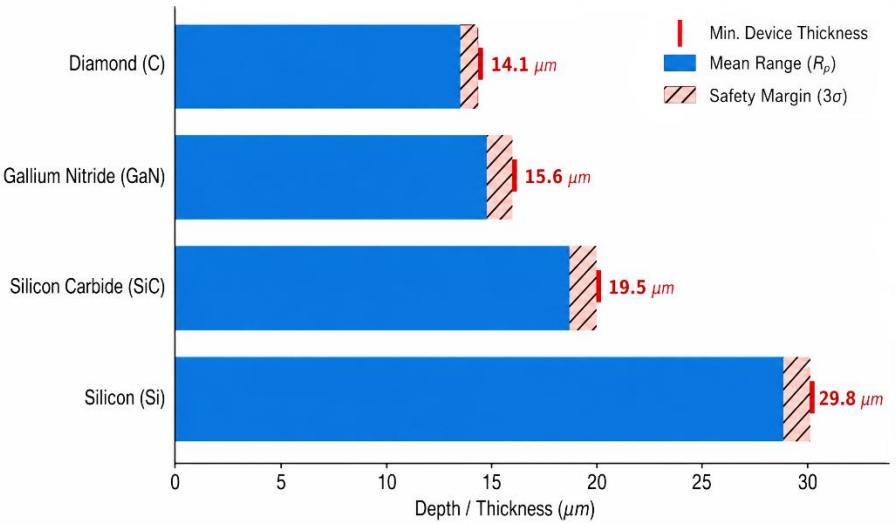

Figure 5. Design the material thickness with a safety margin.

CONCLUSIONS

This study confirms that Am-241 waste is feasible for micro-scale nuclear energy applications, with substrate material selection being a critical factor. Diamond demonstrates the best technical performance, exhibiting the highest Radiation Tolerance Index (670) and the lowest structural damage, making it the most radiation-hard material. However, for large-scale and cost-sensitive applications, SiC is recommended as the optimal compromise due to its high radiation tolerance and mature fabrication technology. In contrast, GaN shows the lowest tolerance ratio, primarily due to enhanced nuclear stopping caused by heavy gallium atoms, which should be carefully considered in GaN-based designs. For practical deployment in Indonesia, particularly for reutilizing detector waste, SiC substrates with an active thickness of around 20 µm are recommended to ensure safe and reliable operation.

AUTHOR CONTRIBUTIONS

PMA: concept the manuscript, conduct simulation, analyse the data. MM: literature review, finalize the manuscript.

REFERENCES

[1] A. Istavara, R. Ratiko, H. A. Pratama, and N. Nasruddin, “Pemodelan Dinamik Pendinginan Bahan Bakar Nuklir Bekas Reaktor Riset Secara Natural Konveksi pada Prototipe Dry Cask,” *Urania :*

Jurnal Ilmiah Daur Bahan Bakar Nuklir, vol. 28, no. 2, p. 113, Jun. 2022, doi: 10.17146/urania.2022.28.2.6639.

[2] P. A. Artiani, Y. Purwanto, A. Aisyah, R. Ratiko, J. Rachmadetin, and K. Heriyanto, "Criticality Safety Analysis of the Dry Cask Design with Air Gaps for RDNK Spent Pebble Fuels Storage," *JURNAL TEKNOLOGI REAKTOR NUKLIR TRI DASA MEGA*, vol. 23, no. 3, p. 123, Sep. 2021, doi: 10.17146/tdm.2021.23.3.6355.

[3] P. O. Oforiwaa, W. Ju., L. Manchun, and S. Guofeng, "DSRS Radioactive Waste Management: A Safety Empirical Assessment For Borehole Disposal System," *The Proceedings of the International Conference on Nuclear Engineering (ICONE)*, vol. 2023.30, no. 0, p. 1012, 2023, doi: 10.1299/jsmeicone.2023.30.1012.

[4] R. Setiawan, K. Megasari, S. Sucipta, and A. Setiawan, "Potensi Lingkungan Kawasan Nuklir Serpong dan Evaluasi Keselamatan Untuk Tapak Fasilitas Borehole Disposal Limbah Sumber Radiasi Bekas," *Urania: Jurnal Ilmiah Daur Bahan Bakar Nuklir*, vol. 29, no. 1, pp. 33–44, Dec. 2024, doi: 10.17146/urania.2023.29.1.6717.

[5] M. T. H. Norman, F. Monado, and M. Ariani, "Analisis Pengaruh Penambahan Minor Aktinida Am-241 dan Np-237 pada Performa Sel Bahan Bakar Uranium Metalic U-10%wtZr," *Jurnal Riset Fisika Indonesia*, vol. 5, no. 2, pp. 86–96, Jun. 2025, doi: 10.33019/jrfi.v5i2.5864.

[6] F. Bouzid, E. Kayahan, M. A. Saeed, B. Babes, S. S. M. Ghoneim, and F. Pezzimenti, "Modeling and simulation of a high power InGaP/GaAs heterojunction alphavoltaic battery irradiated by americium-241," *Semiconductor Physics, Quantum Electronics and Optoelectronics*, vol. 27, no. 02, pp. 224–234, Jun. 2024, doi: 10.15407/spqeo27.02.224.

[7] X. Han, F. Cao, P. Qu, P. Jin, and Z. Wang, "A review for nuclear batteries based on diamond," *Functional Diamond*, vol. 6, no. 1, Dec. 2026, doi: 10.1080/26941112.2025.2601399.

[8] M. Prelas, M. Boraas, F. De La Torre Aguilar, J.-D. Seelig, M. Tchakoua Tchouaso, and D. Wisniewski, *Nuclear Batteries and Radioisotopes*, vol. 56. Cham: Springer International Publishing, 2016. doi: 10.1007/978-3-319-41724-0.

[9] Q. Zhao *et al.*, "Research Progress on Radiation Volt-Effect Isotope Cells," *Carbon Neutralization*, vol. 4, no. 5, Sep. 2025, doi: 10.1002/cnl2.70039.

[10] M. Moll, "Displacement Damage in Silicon Detectors for High Energy Physics," *IEEE Trans. Nucl. Sci.*, vol. 65, no. 8, pp. 1561–1582, Aug. 2018, doi: 10.1109/TNS.2018.2819506.

[11] J. R. Srour and J. W. Palko, "Displacement Damage Effects in Irradiated Semiconductor Devices," *IEEE Trans. Nucl. Sci.*, vol. 60, no. 3, pp. 1740–1766, Jun. 2013, doi: 10.1109/TNS.2013.2261316.

[12] C. E. Munson *et al.*, "Modeling, design, fabrication and experimentation of a GaN-based, ^{63}Ni betavoltaic battery," *J. Phys. D Appl. Phys.*, vol. 51, no. 3, p. 035101, Jan. 2018, doi: 10.1088/1361-6463/aa9e41.

[13] I. Capan, "Wide-Bandgap Semiconductors for Radiation Detection: A Review," *Materials*, vol. 17, no. 5, p. 1147, Mar. 2024, doi: 10.3390/ma17051147.

[14] R. Ponnambalam and I. Vairavasundaram, "GaN-Based DC-DC converters for EV fast charging: A review of wide bandgap devices technology," *Results in Engineering*, vol. 28, p. 107548, Dec. 2025, doi: 10.1016/j.rineng.2025.107548.

[15] M. De Napoli, "SiC detectors: A review on the use of silicon carbide as radiation detection material," *Front. Phys.*, vol. 10, Oct. 2022, doi: 10.3389/fphy.2022.898833.

[16] Satoshi. Koizumi, C. E. . Nebel, and Milos. Nesladek, *Physics and applications of CVD diamond*. Wiley-VCH, 2008.

[17] X. Han, F. Cao, P. Qu, P. Jin, and Z. Wang, "A review for nuclear batteries based on diamond," *Functional Diamond*, vol. 6, no. 1, Dec. 2026, doi: 10.1080/26941112.2025.2601399.

[18] M. Gatchell and H. Zettergren, "Knockout driven reactions in complex molecules and their clusters," *Journal of Physics B: Atomic, Molecular and Optical Physics*, vol. 49, no. 16, p.

162001, Aug. 2016, doi: 10.1088/0953-4075/49/16/162001.

[19] S. Xue, C. Tan, P. Kandlakunta, I. Oksuz, V. Hlinka, and L. R. Cao, “Methods for improving the power conversion efficiency of nuclear-voltaic batteries,” *Nucl. Instrum. Methods Phys. Res. A*, vol. 927, pp. 133–139, May 2019, doi: 10.1016/j.nima.2019.01.097.

[20] T. Gao, A. Zhang, L. Chen, J. Li, C. Liu, and Y. Cui, “Structural design and optimization of 3D interface structures based on betavoltaic nuclear batteries,” *AIP Adv.*, vol. 14, no. 6, Jun. 2024, doi: 10.1063/5.0191142.

[21] J. Lei, N. Wang, R. Jiang, and Q. Hou, “Simulation-Based Analysis of the Effect of Alpha Irradiation on GaN Particle Detectors,” *Micromachines (Basel).*, vol. 14, no. 10, p. 1872, Sep. 2023, doi: 10.3390/mi14101872.

[22] J. F. Ziegler, M. D. Ziegler, and J. P. Biersack, “SRIM – The stopping and range of ions in matter (2010),” *Nucl. Instrum. Methods Phys. Res. B*, vol. 268, no. 11–12, pp. 1818–1823, Jun. 2010, doi: 10.1016/j.nimb.2010.02.091.

[23] K. Nordlund *et al.*, “Primary radiation damage: A review of current understanding and models,” *Journal of Nuclear Materials*, vol. 512, pp. 450–479, Dec. 2018, doi: 10.1016/j.jnucmat.2018.10.027.

[24] G. F. . Knoll, *Radiation detection and measurement*. John Wiley, 2010.

[25] D. Delgado and R. Vila, “Statistical Molecular Dynamics study of displacement energies in diamond,” *Journal of Nuclear Materials*, vol. 419, no. 1–3, pp. 32–38, Dec. 2011, doi: 10.1016/j.jnucmat.2011.08.035.

[26] Z. Q. Ma and Y. Kido, “The atomic displacements on surface generated by low-energy projectile,” *Thin Solid Films*, vol. 359, no. 2, pp. 288–292, Jan. 2000, doi: 10.1016/S0040-6090(99)00742-7.

[27] K. Wu *et al.*, “Anisotropic displacement threshold energy and defect distribution in diamond: PKA energy and temperature effect,” *Chinese Physics B*, vol. 34, no. 8, p. 087104, Aug. 2025, doi: 10.1088/1674-1056/add4f8.

[28] L. A. Miller, D. K. Brice, A. K. Prinja, and S. T. Picraux, “Molecular dynamics simulations of bulk displacement threshold energies in Si,” *Radiation Effects and Defects in Solids*, vol. 129, no. 1–2, pp. 127–131, Jun. 1994, doi: 10.1080/10420159408228889.